ACCSCIENCE PUBLISHING

Green Technology & Innovation

ARTICLE

Experimental investigation on the heating characteristics of a transcritical CO_2 heat pump

Lingxiao Yang[1] and Zhenqian Chen[1,2]*

[1]Key Laboratory of Energy Thermal Conversion and Control of Ministry of Education, School of Energy and Environment, Southeast University, Nanjing, Jiangsu, China

[2]Jiangsu Provincial Key Laboratory of Solar Energy Science and Technology, School of Energy and Environment, Southeast University, Nanjing, Jiangsu, China

Abstract

Inadequately configured operating parameters can have a detrimental effect on the performance of a transcritical CO_2 heat pump due to the unique thermophysical properties of CO_2. This study investigates the heat transfer characteristics of the gas cooler (GC) and the effects of three operating parameters on the heating process of the system. The results showed that: The temperature distribution of CO_2 and water in the GC exhibited typical "two-region" and "three-zone" patterns; and the increase in discharge pressure enhanced the thermal quality of the GC CO_2 side, thereby improving the heat output temperature. Nevertheless, higher thermal quality on the GC CO_2 side can exacerbate the heat capacity mismatch between the two fluids, thereby reducing the system coefficient of performance (COP). Furthermore, increasing compressor speed (n_{com}) mitigated the mismatch in heat capacity caused by elevated thermal quality. Taken together, n_{com} resulted in a 14.7°C increase in heating temperature within the experimental range, accompanied by an 18.4% decrease in COP, showing the best performance among the three parameters studied. This study offers a critical reference for both the theoretical analysis and the control strategy of transcritical CO_2 heat pumps, directly supporting the pursuit of efficient heating.

Keywords: Transcritical CO_2 heat pump; Gas cooler; Compressor speed; Heating performance

***Corresponding author:**
Zhenqian Chen
(zqchen@seu.edu.cn)

Citation: Yang L, Chen Z. Experimental investigation on the heating characteristics of a transcritical CO_2 heat pump. *Green Technol Innov*.
doi: 10.36922/GTI025320011

Received: August 8, 2025

1st revised: October 20, 2025

2nd revised: November 4, 2025

Accepted: November 7, 2025

Published online: November 24, 2025

1. Introduction

Carbon dioxide (CO_2), a greenhouse gas, is an inexpensive, safe, and environmentally friendly natural refrigerant. Given its high critical pressure and low critical temperature, CO_2 heat pumps typically employ transcritical cycles.[1,2] In this cycle, CO_2 releases heat in the gas cooler (GC) during the cooling process. Unlike the condensation process occurring in other heat pumps, the pressures and temperatures of CO_2 in the cooling process are decoupled.[3] Benefiting from this feature, the transcritical CO_2 heat pump (TCHP) exhibits advantages in heating with a significant temperature differential, a feat that is challenging for conventional single-stage heat pumps. In addition, it can provide heating at a higher temperature.[4,5]

Research into GCs—a critical component of a heat pump system—remains active. Within these systems, heat transfer of supercritical CO_2 can be effectively modeled as a

constant-pressure cooling event.[6] Previous analyses of CO_2 heat transfer have identified a near-critical temperature range and associated region[7] (Figure 1). Within this near-critical zone, CO_2's isobaric lines are nearly horizontal near the critical temperature point. However, as the temperature deviates from this range, the isobars become progressively steeper. This behavior results in a highly variable distribution of CO_2's specific heat capacity during cooling in the GC. The heat capacity peaks within the near-critical zone and diminishes significantly outside it.[8,9]

The non-uniform heat capacity distribution of CO_2 significantly influences the performance of the GC. Research by Chen *et al.*[10] demonstrated that increasing the heat transfer surface area within the GC does not always lower the temperature approach difference. In a further study on system optimization, Chen *et al.*[11] incorporated pinch point effects and refined prediction methods to study optimal discharge pressure. Parallel work by Ye *et al.*[12] also utilized pinch point analysis to determine the optimal discharge pressure in a TCHP featuring an internal heat exchanger. Cui *et al.*[13] and Cui *et al.*[13,14] explored the pinch point behaviors in a CO_2–water GC across diverse operating parameters, with experimental data confirming their findings. This investigation revealed four distinct patterns of pinch point movement and established two key relationships linking optimal discharge pressure to pinch point location. In addition, enhanced thermal matching at lower water inlet temperatures correlated with improved system efficiency (higher coefficient of performance [COP]). However, no such efficiency gain from thermal matching was observed at elevated water inlet temperatures.

The actual heat exchange in a GC corresponds to its heat transfer area. Due to the continuous variation in the temperature difference for heat exchange, the temperature change patterns on the CO_2 side and the water side during a GC heat transfer process are not constant. Although existing pinch point studies can identify key phenomena in the heat exchange process, they do not truly reflect the actual heat transfer processes within the GC. These limitations underscore the need for more in-depth experimental research. Accordingly, the present study examines the heat transfer performance of an enhanced GC design and evaluates the effects of three key operating parameters on the system's heating behavior. The findings provide valuable insights into both the theoretical modeling and control strategy development of TCHPs, while also offering practical guidance for GC design optimization.

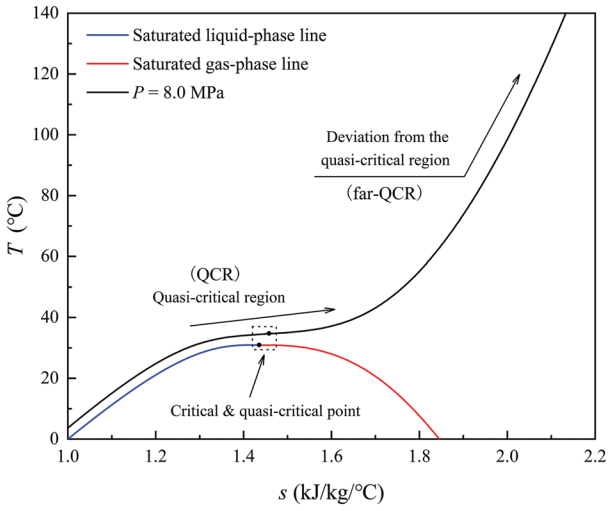

Figure 1. The temperature (T)–entropy (s) diagram of CO_2

2. Methodology

2.1. Test prototype

As shown in Figure 2, the test apparatus consisted of a set of water-source TCHP system. The simplified flowchart is depicted in Figure 3. Compared with the basic TCHP cycle, this system incorporated an enhanced GC design with a "three-stage" configuration. To conduct a detailed investigation into the process of GC heat transfer, three modified GCs based on the SS-0100GN-U (Shenshi Technology, China) with identical specifications were arranged in a configuration that followed the direction of the water flow. These coolers were named GC-1, GC-2, and GC-3 for the purpose of this study. Temperature measurements were obtained using eight thermocouples (PT100-A50, KAIPUSEN, China). This instrumentation enabled the implementation of a segmented GC configuration, featuring three thermally distinct stages with equal surface areas, each representing one-third of the total heat exchange surface.

Figure 2. The prototype of the experiment

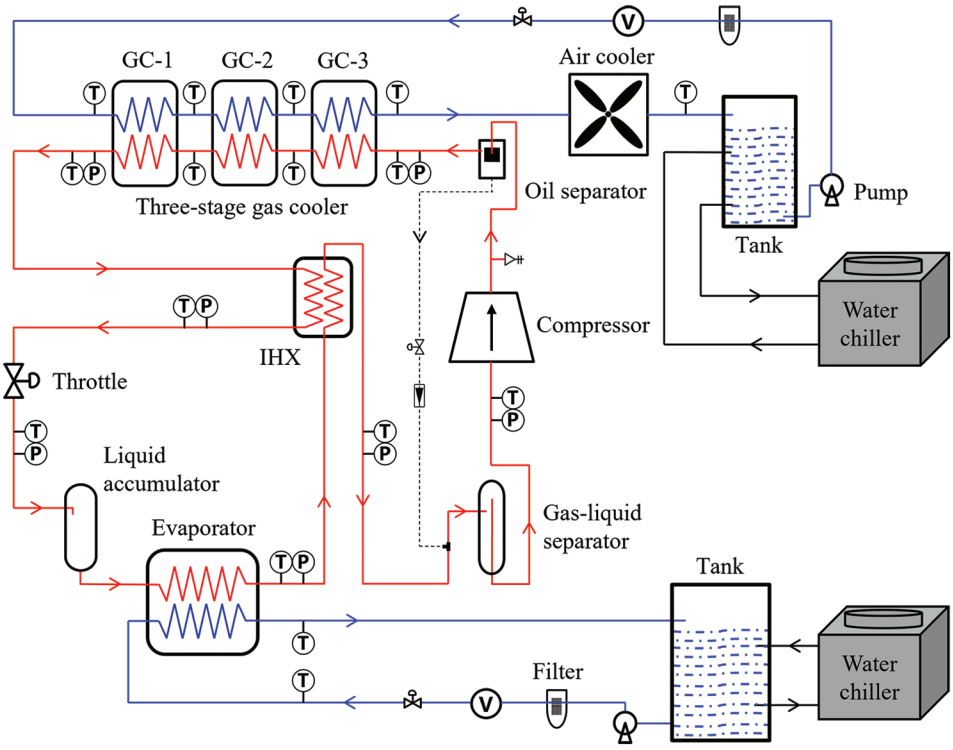

Figure 3. Diagram of the experimental bench
Abbreviations: GC: Gas cooler; IHX: Internal heat exchanger.

Table 1 lists the main experimental components, and Table 2 summarizes the specifications of the measuring devices.

2.2. Data reduction

The heating capacity (Q_h) of the system was estimated using Equation (1):

$$Q_h = V_{w,gc} \cdot \rho_w \cdot c_{p,w} \cdot \Delta T_{w,gc} \quad (1)$$

where $V_{w,gc}$ is the GC water flow (m³/s), ρ_w is the water density (kg/m³), $c_{p,w}$ is the water specific heat capacity (kJ/kg/°C), and $\Delta T_{w,gc}$ is the inlet and outlet temperature difference of water in GC (°C)

The COP of the system was calculated using Equation (2):

$$COP = \frac{Q_h}{P} \quad (2)$$

where P is the power consumption by the compressor (kW).

The measurement uncertainty was calculated using the method proposed by Kline and McClintock,[15] with the uncertainty of Q_h estimated at a maximum of 1.90% and the uncertainty of COP at a maximum of 2.15%.

Table 1. Key experimental components

Components	Characteristics
Compressor	C-CV153HOP (Panasonic, China) Twin-rotor; Rated power: 0.9 kW; Speed ranges: 37–100 rps
GC	Tube-in-tube (TIT); Length: 4.5×3 m
IHX	TIT
Evaporator	TIT
Expansion	Manual throttle
Oil separator	Temprite-131 (Temprite, USA)
Liquid accumulator	Customization
Gas-liquid separator	Customization

Abbreviations: GC: Gas cooler; IHX: Internal heat exchanger.

2.3. Experimental design

For a TCHP, regulating the throttle opening leads to a typical working condition known as the optimal COP condition (COP_{opt}), where the system achieves its best performance.[16,17] Operating parameters significantly influence system performance, with three primary operational parameters identified: Compressor speed (n_{com}), GC water inlet flow rate ($V_{w,gc,in}$), and GC water

inlet temperature ($T_{w,gc,in}$). Under a constant ambient heat-source temperature (T_{am}), this study comprised two parts, with the experimental designs summarized in Table 3.

The first part focused on GC heat exchange based on Case 6 in Table 3, using the representative COP_{opt} condition as the reference case. The second part addressed the effects of the three operating parameters on system heat output performance. Five distinct experimental designs were developed for each parameter: Cases 1–5 examined n_{com}, Cases 6–10 evaluated $V_{w,gc,in}$, and Cases 11–15 assessed $T_{w,gc,in}$. Each case used the COP_{opt} condition as a baseline.

During the experimental process, the discharge pressure (p_{dis}) was adjusted by changing the throttle opening to identify the optimal p_{dis} ($p_{dis,opt}$) corresponding to COP_{opt}. After every adjustment to the throttle opening, the system required more than 20 min to stabilize. Each operating condition was tested twice to enable comparison. Although variations occurred in the water temperatures entering the GC or evaporator, the control system, employing opposing heating and cooling loops, maintained these fluctuations within ±0.2°C. In addition, water flow into the GC or evaporator was recorded at 2-s intervals, with the final flow value averaged over nearly 5 min.

It is worth noting that the GC heat transfer analysis in Section 3.1 and the parametric analysis in Sections 3.2–3.4 are all based on operating conditions with optimized throttle valve openings. We conducted the GC heat transfer analysis first, then extended it to other operating parameters. Since no single standard exists for optimization, further evaluation combining system-specific metrics, such as heating temperature, is necessary, which will be addressed in future work.

Table 2. Measurement accuracy of the experiment parameters

Parameter	Types	Range	Accuracy
Temperature	T-type thermocouple (Kaipusen, T-type, China)	−60–200°C	±0.5°C
Pressure	Pressure transducer (Meacon, P300G, China)	0–10 MPa	±0.2%
	Pressure transducer (Meacon, P300G, China)	0–20 MPa	±0.2%
Water volume flow	Gear flowmeter (Wuteng, WT02, China)	20–500 L/h	±0.5%
	Gear flowmeter (Wuteng, WT02, China)	50–1,200 L/h	±0.5%
Electric power	Power meter (UNI-T, UTE9800, China)	0–12 kW	± (0.5% of reading+range)

Table 3. Test conditions

Parameter	Case	Variable	Fixed parameters
n_{com}	1	65 rps	T_{am}=28°C; $T_{w,gc,in}$=15°C; $V_{w,gc,in}$=40 L/h
	2	70 rps	
	3	75 rps	
	4	80 rps	
	5	85 rps	
$V_{w,gc,in}$	6	30 L/h	T_{am}=28°C; $T_{w,gc,in}$=15°C; n_{com}=70 rps
	7	35 L/h	
	8	40 L/h	
	9	45 L/h	
	10	50 L/h	
$T_{w,gc,in}$	11	10°C	T_{am}=28°C; n_{com}=70 rps; $V_{w,gc,in}$=40 L/h
	12	15°C	
	13	20°C	
	14	25°C	
	15	30°C	

3. Results and discussion

3.1. Heat exchange characteristics of the gas cooler

In this section, we introduce the concepts of heat capacity and thermal quality. Heat capacity denotes the ability of a fluid to absorb or release heat and is closely related to its specific heat and mass flow rate. Thermal quality represents the extent of heat released on the CO_2 side during the GC heat transfer process and corresponds to CO_2 temperature. Next, the impact of throttle opening changes on the system is explained.

When the throttle was narrowed, the mass flow rate of CO_2 progressively declined. This redistribution shifted some of the retained CO_2 from the low-pressure side to the high-pressure side, causing evaporation pressure to drop and discharge pressure to rise. However, other studies[18,19] indicate that the relationship between throttle restriction and mass flow reduction is non-linear. In the initial phase of throttling, the rise in CO_2 velocity through the valve can partly counteract the effect of the smaller opening on mass flow.

In the following study, we assessed the heat transfer characteristics of the GC and the influence of key system parameters by adjusting the throttle opening to the reference COP_{opt} condition. In addition, in accordance with the established experimental operating conditions (Case 6 in Table 3) and the COP_{opt} condition, temperature changes during GC heat exchange were investigated.

Figure 4 reveals a characteristic two-phase temperature progression for CO_2. Following compressor discharge, CO_2 entered the GC for cooling. Initially residing in the far quasi-critical region (QCR)—where its temperature substantially exceeded the pressure-dependent quasi-

critical threshold—the fluid demonstrated high thermal quality but low heat capacity. As cooling progressed and the CO_2 temperature approached the quasi-critical value, its transition to the QCR occurred. Within QCR, CO_2 exhibited opposite characteristics: Low thermal quality coupled with high heat capacity.

Unlike CO_2, the heat capacity of water in the GC showed minimal temperature-dependent variation under the experimental conditions. The dual-region behavior of CO_2 induced tripartite water temperature progression in the GC, labeled GC-1, GC-2, and GC-3.

i. Zone GC-1 (Stage 1): The temperature difference between the two fluids was large, and the isobaric heat capacity of CO_2 in QCR far exceeded that of water. Consequently, the temperature of CO_2 changed less markedly than that of water. During this phase, water temperature rose rapidly while CO_2 temperature increased gradually (following water's trajectory), driving swift thermal convergence.
ii. Zone GC-2 (Stage 2): Once the fluid temperatures approached each other, the process entered a second regime. Although CO_2 still possessed a higher heat capacity, its limiting effect on the water temperature became evident: The slope of the water temperature curve flattened, and the convergence rate dropped.
iii. Zone GC-3 (Stage 3): As CO_2 drifted out of the QCR, its heat capacity fell below that of water. The roles were reversed, with water now buffering temperature change. As a result, the temperature difference between the two fluids began to widen again.

We achieved a three-stage, equal-area cooling of CO_2 at the compressor outlet using three GCs of the same specification. Since the water flow rate entering the GCs remained constant throughout the experiment, the water temperature changes, as shown in Figure 4, were entirely translated into variations in the heat transferred by the water as it passed successively through the three equal-area GCs. As a result, in Stage 1, due to the higher initial heat exchange temperature difference, the corresponding heat exchange of the water was the highest. In Stages 2 and 3, as the heat exchange temperature difference decreased, the corresponding heat exchange was significantly lower than in Stage 1, leading to a noticeable change in the slope of the water temperature rise across the GCs.

3.2. Effects of compressor speed

Figure 5 presents the effects of n_{com} on the COP_{opt}, $Q_{h,opt}$, and $p_{dis,opt}$ of the system based on Cases 1–5 in Table 3. As shown, COP_{opt} decreased as n_{com} increased. When n_{com} rose from 65 rps to 85 rps, COP_{opt} declined from 2.65 to 2.16, an 18.4% drop. Conversely, both $Q_{h,opt}$ and $p_{dis,opt}$ increased with n_{com}; $Q_{h,opt}$ increased from 2.84 kW to 3.54 kW, and $p_{dis,opt}$ increased steadily from 9.45 MPa to 10.31 MPa. The variation in COP_{opt} can be explained from both thermodynamic and heat transfer viewpoints. Thermodynamically, the evaporation pressure of the system remains relatively stable under constant T_{am} conditions. However, $p_{dis,opt}$ increases as n_{com} rises, leading to a broader range of operating conditions. This expansion was identified as the primary factor contributing to the decline in COP_{opt}. From the heat transfer perspective, increasing n_{com} raises the mass flow rate of CO_2 circulating through the system. This enhances the heat transfer and Q_h at the GC, thereby partially mitigating the reduction in COP_{opt}.

The temperature variation in the GC under different levels of n_{com} is shown in Figure 6. As n_{com} increased, the

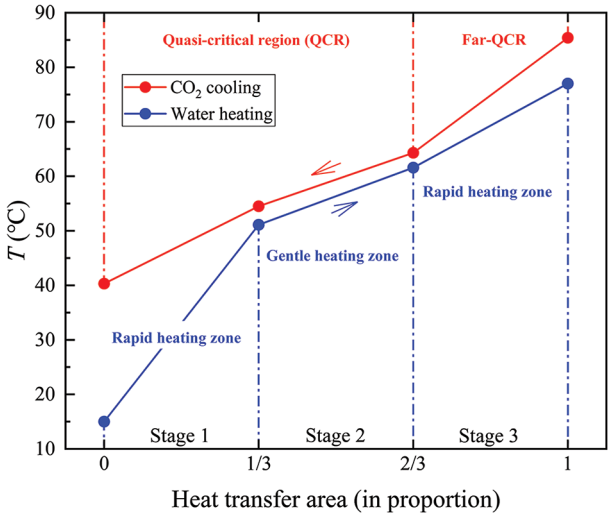

Figure 4. Heat exchange process of the gas cooler

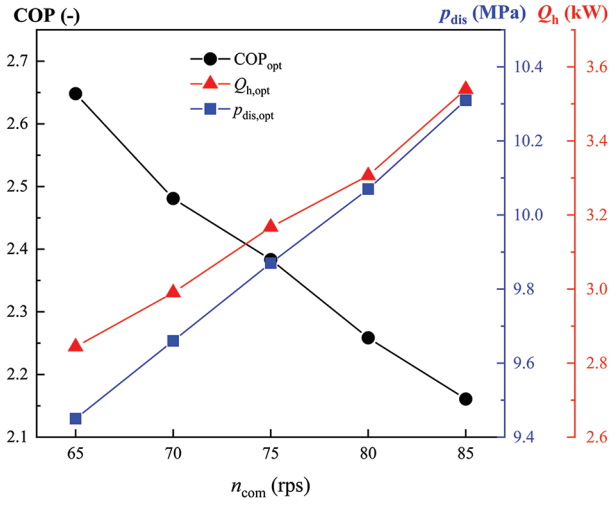

Figure 5. Changes in $p_{dis,opt}$, $Q_{h,opt}$, and COP_{opt} of the cycle with n_{com}

temperature curve of the cooled CO_2 elevated noticeably. It is imperative to note that the water temperature at the outlet of each stage also increased correspondingly. Moreover, $p_{dis,opt}$ rose with increasing n_{com}, indicating an elevation in CO_2's quasi-critical temperature during GC operation, thereby enhancing the thermal quality within the QCR. Consequently, a higher heating temperature was achieved. At the same time, the increase in n_{com} markedly increased the mass flow rate of CO_2 flowing through the GC, thereby enhancing the heat capacity on the CO_2 side.[20,21] However, since the operating conditions on the water side remained constant, this additional heat capacity on the CO_2 side could not be fully transferred to the water side, leading to an increase in the corresponding CO_2 outlet temperature in the GC. This led to an increased heat capacity mismatch in the GC, negatively affecting the heating performance of the system. Notably, the elevation of the CO_2 mass flow rate also enhanced the heat transfer performance on the CO_2 side, partially mitigating the negative effects of heat capacity mismatch within the GC.

3.3. Effects of the water inlet flow rate of the gas cooler

The changes in $p_{dis,opt}$, $Q_{h,opt}$, and COP_{opt} of the cycle at different $V_{w,gc,in}$ are shown in Figure 7 (Cases 6–10 shown in Table 3). As presented, COP_{opt} dropped with decreasing $V_{w,gc,in}$. Specifically, as $V_{w,gc,in}$ dropped from 50 L/h to 30 L/h, COP_{opt} declined from 2.95 to 2.00, a drop of 32.2%. In addition, as $V_{w,gc,in}$ decreased, $Q_{h,opt}$ declined while $p_{dis,opt}$ increased. As $V_{w,gc,in}$ declined from 50 L/h to 30 L/h, $Q_{h,opt}$ dropped from 3.36 kW to 2.62 kW, a decrease of 21.9%, and $p_{dis,opt}$ rose from 9.19 MPa to 10.41 MPa. The variation in COP_{opt} can also be explained through thermodynamic and heat transfer analyses. Thermodynamically, a decrease in $V_{w,gc,in}$ results in an increase in $p_{dis,opt}$ and a broader operational range, both of which negatively affect system performance. From a heat transfer standpoint, the reduction in $V_{w,gc,in}$ weakens heat transfer efficiency on the water side, further accelerating the decline in COP_{opt}.

The temperature variation in the GC under different levels of $V_{w,gc,in}$ is shown in Figure 8. As $V_{w,gc,in}$ decreased, the overall curves of the cooled CO_2 were significantly elevated, enabling the system to reach higher heating temperatures. Similar to the effects of n_{com}, this phenomenon was attributed to the rise in $p_{dis,opt}$, indicating that reducing $V_{w,gc,in}$ improves the CO_2 thermal level during GC heat exchange processes. In addition, reducing $V_{w,gc,in}$ decreases

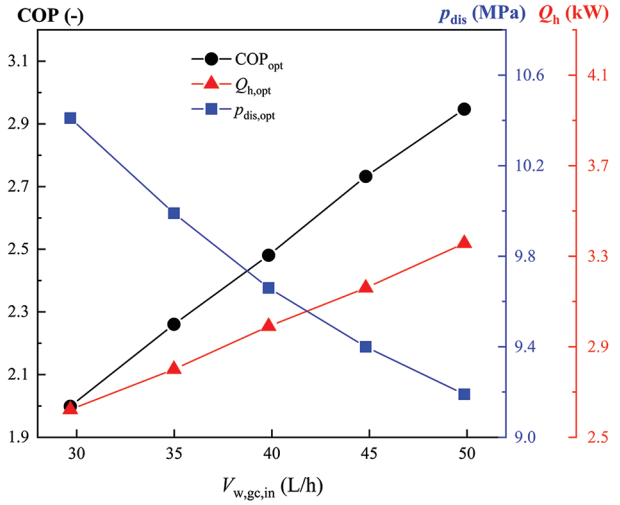

Figure 7. Changes in $p_{dis,opt}$, $Q_{h,opt}$, and COP_{opt} of the cycle with $V_{w,gc,in}$

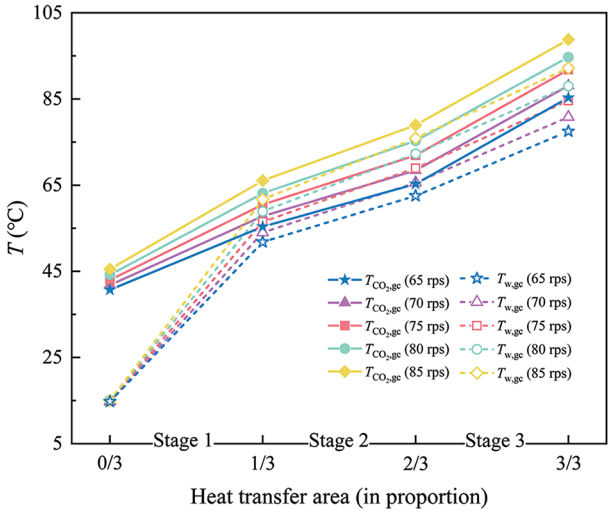

Figure 6. Temperature variation on both sides of the GC under different n_{com} levels

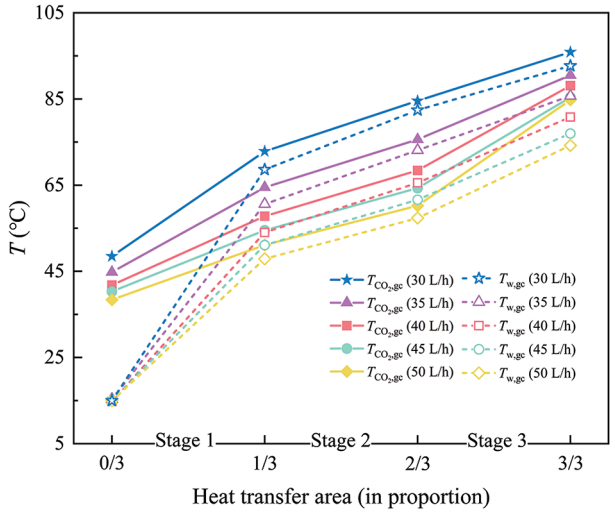

Figure 8. Temperature variation on both sides of the GC under different $V_{w,gc,in}$ levels

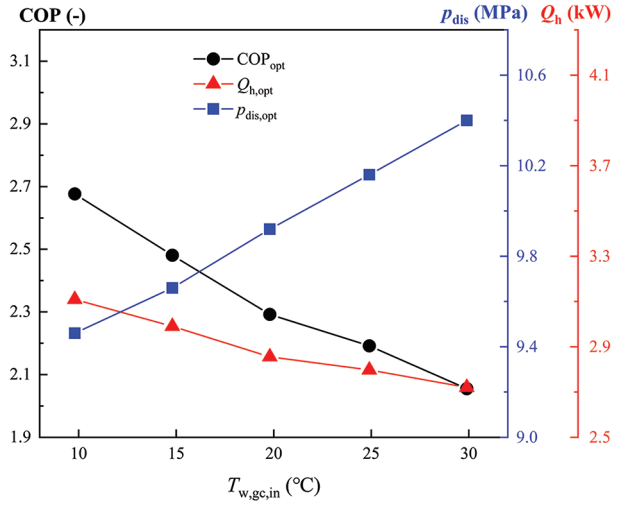

Figure 9. Changes in $p_{dis,opt}$, $Q_{h,opt}$, and COP_{opt} of the cycle with $T_{w,gc,in}$

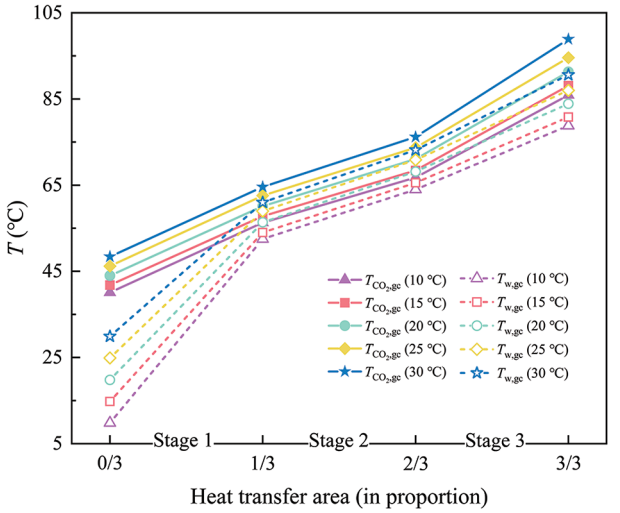

Figure 10. Temperature variation on both sides of the GC under different $T_{w,gc,in}$ levels

the water-side heat capacity. Specifically, the water's heat absorption capability at Stage 1 diminished proportionally to CO_2 heat rejection. This decline in heat release increased the CO_2 outlet temperature in the GC. Therefore, reducing $V_{w,gc,in}$ negatively affects the matching of heat capacity between both sides of the GC. Moreover, the variation in $V_{w,gc,in}$ showed a significantly greater influence on the CO_2 outlet temperature and the system performance compared to the variation in n_{com}. The main reason for this is that decreasing $V_{w,gc,in}$ degrades heat transfer in the GC, whereas increasing n_{com} enhances it.

3.4. Effects of the water inlet temperature of the gas cooler

Changes in $p_{dis,opt}$, $Q_{h,opt}$, and COP_{opt} of the cycle at different $T_{w,gc,in}$ are shown in Figure 9 (Cases 11–15 shown in Table 3). As shown, COP_{opt} decreased with rising $T_{w,gc,in}$: As $T_{w,gc,in}$ elevated from 10°C to 30°C, COP_{opt} decreased from 2.68 to 2.06, a 23.2% drop. In addition, as $T_{w,gc,in}$ increased, $Q_{h,opt}$ decreased while $p_{dis,opt}$ increased. As $T_{w,gc,in}$ increased from 10°C to 30°C, $Q_{h,opt}$ dropped from 3.11 kW to 2.72 kW, a 12.5% decrease, and $p_{dis,opt}$ increased from 9.46 MPa to 10.40 MPa. The thermodynamic explanation for the COP_{opt} decline lies in the concurrent increase in $p_{dis,opt}$ and the broadening of operational conditions induced by a higher $T_{w,gc,in}$. From the heat transfer viewpoint, a higher $T_{w,gc,in}$ shrinks the temperature difference within the GC. This diminished gradient directly impedes efficient heat rejection, thereby contributing to the reduction in COP_{opt}.

The temperature variations in the GC under different $T_{w,gc,in}$ are shown in Figure 10. As shown, the overall temperature profile of the cooled CO_2 clearly increased as $T_{w,gc,in}$ elevated, and the corresponding water temperatures also increased, which was again due to the rise in $p_{dis,opt}$. This indicates that an increase in $T_{w,gc,in}$ positively influences the thermal quality of CO_2, enabling the system to achieve higher heating temperatures. Similar to the effects of $V_{w,gc,in}$, an increase in $T_{w,gc,in}$ directly reduced the amount of heat the water could absorb at the end of Stage 1. Influenced by this, the heat released by CO_2 at this stage decreases, leading to a higher CO_2 outlet temperature in the GC. Therefore, increasing $T_{w,gc,in}$ adversely affects the heat capacity matching during the GC heat exchange processes.

4. Conclusion

In this study, the heat exchange characteristics of the GC were evaluated, and the effects of three operating parameters on the heating process of the system were investigated from the viewpoint of thermal quality and heat capacity. The key findings of this study are summarized below:

(i) During heat transfer in the GC, the temperatures of CO_2 and water exhibit characteristic "two-region" and "three-zone" distribution patterns, respectively. An increase in cooling pressure on the CO_2 side enhances the CO_2 thermal quality, thereby increasing the heating temperature of the system.

(ii) An increase in n_{com}, a decrease in $V_{w,gc,in}$, and an increase in $T_{w,gc,in}$ can result in higher $p_{dis,opt}$ and increased CO_2 outlet temperature in the GC. In general, the elevated thermal quality on the GC CO_2 side exacerbates the heat capacity mismatch between the two sides, further adversely affecting the system's COP. In addition,

increasing n_{com} mitigates this mismatch, while decreasing $V_{w,gc,in}$ and rising $T_{w,gc,in}$ worsen it.

(iii) Within the experimental range, increasing n_{com} results in a 14.7°C increase in the heating temperature, accompanied by an 18.4% decrease in COP and a 24.4% increase in Q_h. Reducing $V_{w,gc,in}$ leads to an 18.5°C rise in the system heating temperature at the cost of a 32.2% and 21.9% drop in COP and Q_h, respectively. Increasing $T_{w,gc,in}$ causes an 11.8°C increase in heating temperature, with a 23.2% decrease in COP and a 12.5% drop in Q_h. Overall, n_{com} exhibited the best performance for increasing heating temperature among the three parameters studied.

In this study, the analysis of system performance mainly focused on variations in COP and Q_h. However, heating temperature, a key evaluation metric, was not thoroughly examined. Therefore, future work will involve dedicated experiments to further investigate the impact of heating temperature on system performance.

Acknowledgments

None.

Funding

This study was funded by the National Key Technologies Research and Development Program of China (Grant No. 2024YFB4007400).

Conflict of interest

The authors declare that they have no competing interests.

Author contributions

Conceptualization: Zhenqian Chen
Formal analysis: Zhenqian Chen
Investigation: Lingxiao Yang
Methodology: Zhenqian Chen
Writing – original draft: Lingxiao Yang
Writing – review & editing: Lingxiao Yang

Ethics approval and consent to participate

Not applicable.

Consent for publication

Not applicable.

Availability of data

The data that support the findings of this study are available from the corresponding author upon reasonable request.

References

1. Dai B, Qi H, Dou W, *et al.* Life cycle energy, emissions and cost evaluation of CO_2 air source heat pump system to replace traditional heating methods for residential heating in China: System configurations. *Ener Conv Manag.* 2020;218:112954.

   doi: 10.1016/j.enconman.2020.112954

2. Ge TS, Weng ZC, Huang R, Hu B, Eikevik TM, Dai YJ. High temperature transcritical CO_2 heat pump with optimized tube-in-tube heat exchanger. *Energy*. 2023;283:129223.

   doi: 10.1016/j.energy.2023.129223

3. Liao SM, Zhao TS, Jakobsen A. A correlation of optimal heat rejection pressures in transcritical carbon dioxide cycles. *Appl Ther Eng*. 2000;20(9):831-841.

   doi: 10.1016/S1359-4311(99)00070-8

4. Lorentzen G. Revival of carbon dioxide as a refrigerant. *Int J Refriger*. 1994;17(5):292-301.

   doi: 10.1016/0140-7007(94)90059-0

5. Song Y, Cui C, Yin X, Cao F. Advanced development and application of transcritical CO_2 refrigeration and heat pump technology-a review. *Ener Rep.* 2022;8:7840-7869.

   doi: 10.1016/j.egyr.2022.05.233

6. Liu R, Gao F, Liang K, *et al.* Thermodynamic evaluation of transcritical CO_2 heat pump considering temperature matching under the constraint of heat transfer pinch point. *J Therm Sci*. 2021;30(3):869-879.

   doi: 10.1007/s11630-021-1373-z

7. Wang X, Yang L, Xu B, Chen Z. Analysis of coupled heat transfer and flow behaviors of supercritical CO_2 in horizontal circular tube. *Int J Heat Fluid Flow*. 2026;117:110064.

   doi: 10.1016/j.ijheatfluidflow.2025.110064

8. Zhao W, Zhang Y, Sun C, Li L, Li B, Xu J. Thermodynamic analysis of a transcritical CO_2 heat pump for heating applications. *Energy*. 2025;318:134896.

   doi: 10.1016/j.energy.2025.134896

9. Zou H, Li X, Tang M, *et al.* Temperature stage matching and experimental investigation of high-temperature cascade heat pump with vapor injection. *Energy*. 2020;212:118734.

   doi: 10.1016/j.energy.2020.118734

10. Chen YG. Pinch point analysis and design considerations of CO_2 gas cooler for heat pump water heaters. *Int J Refriger*. 2016;69:136-146.

    doi: 10.1016/j.ijrefrig.2016.05.003

11. Chen YG. Optimal heat rejection pressure of CO_2 heat pump water heaters based on pinch point analysis. *Int J Refriger*. 2019;106:592-603.

    doi: 10.1016/j.ijrefrig.2019.04.003

12. Ye Z, Wang Y, Song Y, Yin X, Cao F. Optimal discharge pressure in transcritical CO_2 heat pump water heater with internal heat exchanger based on pinch point analysis. *Int J Refriger*. 2020;118:12-20.

doi: 10.1016/j.ijrefrig.2020.06.003

13. Cui Q, Wei D, Gao E, Zhang X. Compressor control strategy for CO_2 heat pump toward efficient and stable domestic hot water production: An experimental investigation. *Therm Sci Eng Prog*. 2023;38:101681.

doi: 10.1016/j.tsep.2023.101681

14. Cui Q, Wang C, Gao E, Zhang X. Pinch point characteristics and performance evaluation of CO_2 heat pump water heater under variable working conditions. *Appl Therm Eng*. 2022;207:118208.

doi: 10.1016/j.applthermaleng.2022.118208

15. Kline S, McClintock F. Describing uncertainties in single-sample experiments. *J Mech Eng*. 1998;1:3-17.

doi: 10.1016/0894-1777(88)90043-X

16. Yang L, Qin X, Zhao L, Ye S, Wei X, Zhang D. Analysis and comparison of influence factors of hot water temperature in transcritical CO_2 heat pump water heater: An experimental study. *Energy Conv Manag*. 2019;198:111836.

doi: 10.1016/j.enconman.2019.111836

17. Yang LX, Wei XL, Zhao LH, Qin X, Zhang DW. Experimental study on the effect of compressor frequency on the performance of transcritical CO_2 heat pump system with regenerator. *Appl Therm Eng*. 2019;150:1216-1223.

doi: 10.1016/j.applthermaleng.2019.01.091

18. Badache M, Ouzzane M, Eslami-Nejad P, Aidoun Z. Experimental study of a carbon dioxide direct-expansion ground source heat pump (CO_2-DX-GSHP). *Appl Therm Eng*. 2018;130:1480-1488.

doi: 10.1016/j.applthermaleng.2017.10.159

19. Rabelo SN, Paulino TF, Duarte WM, Maia AAT, Machado L. Experimental analysis of the influence of the expansion valve opening on the performance of the small size CO_2 solar assisted heat pump. *Solar Ener*. 2019;190:255-263.

doi: 10.1016/j.solener.2019.08.013

20. Liu X, Wang D, Peng X, Wang G, Yang Y. Experimental study on performance and compressor characteristics of transcritical CO_2 heat pump system. *Appl Therm Eng*. 2024;250:123524.

doi: 10.1016/j.applthermaleng.2024.123524

21. Baek C, Heo J, Jung J, Cho H, Kim Y. Optimal control of the gas-cooler pressure of a CO_2 heat pump using EEV opening and outdoor fan speed in the cooling mode. *Int J Refriger*. 2013;36(4):1276-1284.

doi: 10.1016/j.ijrefrig.2013.02.009